

**STRATIGRAPHIC CONTEXT OF PHYLLOSILICATE DEPOSITS IN SINUS MERIDIANI, MARS.** S. M. Wiseman<sup>1</sup>, R. E. Avidson<sup>1</sup>, F. Poulet<sup>2</sup>, R. V. Morris<sup>3</sup>, S. Murchie<sup>4</sup>, F. P. Seelos<sup>4</sup>, J. C. Andrews-Hanna<sup>5</sup>, and the CRISM Science Team. <sup>1</sup>Dept of Earth and Planetary Sciences, Washington University, St. Louis, MO (sandra@levee.wustl.edu), <sup>2</sup>Institut d' Astrophysique Spatiale (IAS), Orsay, France, <sup>3</sup>NASA Johnson Space Center, Houston, TX, <sup>4</sup>Applied Physics Laboratory, Laurel, MD, <sup>5</sup>Dept of Geophysics, Colorado School of Mines, CO.

**Introduction:** Extensive sedimentary deposits [e.g., 1,2] previously mapped as etched (ET) terrain are exposed in the Sinus Meridiani region. The hematite-bearing plains unit (Ph) explored by the MER rover Opportunity covers portions of the ET (Fig. 1). Dissected cratered terrain (DCT) is exposed to the south of these deposits. Fe/Mg phyllosilicates and hydrated Mg sulfate deposits are detected in Meridiani using both Mars Express OMEGA [3] and MRO CRISM [4] near infrared spectral data [e.g., 5,6,7,8]. We are mapping the spatial distribution of both phyllosilicate and hydrated sulfate deposits within the Sinus Meridiani region using high resolution CRISM images. This work builds on previous studies [e.g., 6,9] and provides a stratigraphic context for the phyllosilicate deposits.

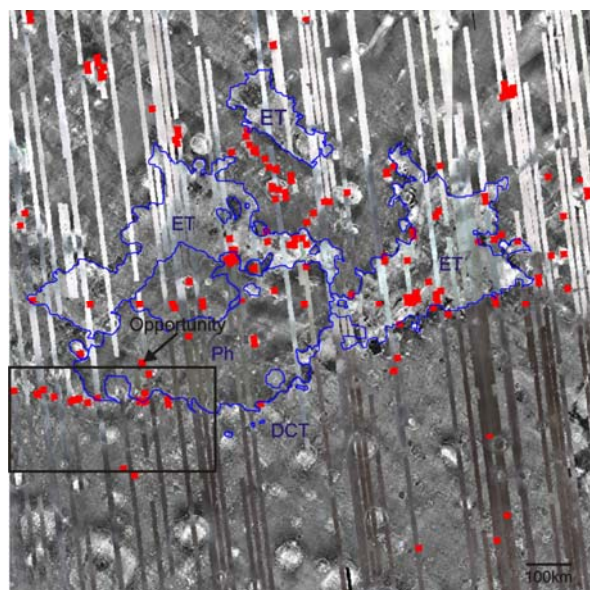


Figure 1. CRISM multispectral survey coverage (R=2.5, G=1.5, B=1.1  $\mu\text{m}$ ) overlain on a THEMIS nighttime IR mosaic. The context map extends from (10°N, 10°W) to (10°S, 10°E). CRISM high resolution targeted footprints are shown in red. Units similar to those mapped by [10] are indicated.

**Fe/Mg Phyllosilicates:** The DCT is a complex unit that contains fluvial features and buried and exhumed craters, some of which exhibit light toned layering [11]. Ph embays DCT along the southern boundary (Fig. 2). Phyllosilicate deposits are exposed within the DCT and occur in close proximity to the Ph

unit in some areas. Detailed examination of these deposits revealed a stratigraphic relationship between the phyllosilicate-bearing deposits and Ph. In Miyamoto crater (Fig. 2), phyllosilicate-bearing deposits are located within ~30 km of the edge of Ph [11], which is presumably underlain by sulfate-rich deposits similar to those explored by the Opportunity rover. The deposits within Miyamoto crater are exposed only in areas where significant exhumation has occurred. The majority of the phyllosilicate exposures in the DCT (Fig. 2) exhibit spectral absorption features at 1.9, 2.3 and 2.4  $\mu\text{m}$ , consistent with the presence of Fe/Mg phyllosilicates [9].

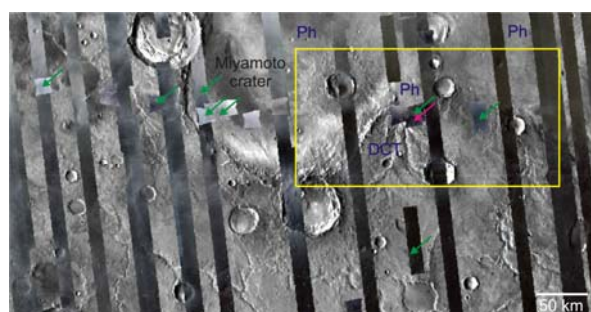


Figure 2. THEMIS daytime IR mosaic of the box shown in Fig. 1 with CRISM multispectral and high resolution coverage overlain (R=2.5, G=1.5, B=1.1  $\mu\text{m}$ ). Areas that are indicated with green arrows exhibit CRISM spectra that are consistent with the presence of Fe/Mg phyllosilicates and the area indicated with a red arrow contains Al-rich phyllosilicates.

**Al-Rich Phyllosilicates:** We have identified Al-rich phyllosilicates, including montmorillonite and kaolinite (Figs. 5,6), for the first time in the Sinus Meridiani region. Fe/Mg smectites are also present in association with the Al-rich phyllosilicates. The phyllosilicate exposures occur within an in place bedrock unit that has been incised via fluvial erosion (Figs. 3,4). Similar phyllosilicate assemblages are found in exposures identified in Mawrth Vallis [e.g., 12]. These deposits occur within the DCT, close to the boundary with Ph (Fig 3). After formation, the phyllosilicate deposits were incised via fluvial erosion [Fig. 4]. Analysis of image and elevation data show that the younger Ph unit embays the phyllosilicate deposits [Fig. 4]. These exposures demonstrate that the phyllosilicate-bearing deposits predate the formation of Ph.

**ET Phyllosilicates:** Both hydrated sulfate and phyllosilicate exposures are identified in association with the ET [e.g., 6,7,8]. The geologic context of these deposits is difficult to decipher because the exposures represent erosional surfaces and are partially buried by mantling material in some areas. Within ET, the phyllosilicate and hydrated sulfate deposits occur in close proximity in some areas. Our current analyses focus on deciphering the stratigraphic relationship between these phyllosilicate and hydrated sulfate deposits.

**Discussion:** Detailed examination of the Al-rich and Mg/Fe phyllosilicate exposures within the DCT show that the phyllosilicate-bearing deposits predate the formation of the Ph unit explored by the Opportunity rover. The deposits record the transition from fluvial conditions which produced and/or preserved phyllosilicates deposits to a progressively acid sulfate dominated groundwater system in which large accumulations of sulfate-rich evaporites were deposited.

The stratigraphic relationship between the phyllosilicate and hydrated sulfate deposits is less clear within the ET. The geochemical conditions experienced by ET at various locations were driven by ground water recharge and evaporative loss rates [13]. Continued mapping of the distribution of phyllosilicate and hydrated sulfate deposits will help to elucidate the aqueous history of the Sinus Meridiani region.

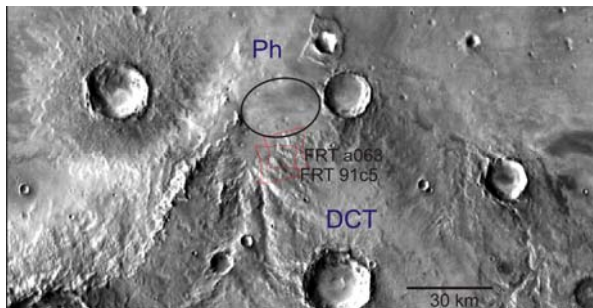


Figure 3. THEMIS daytime IR mosaic of the box shown in Fig. 2. The MSL candidate Southern Meridiani landing ellipse and CRISM FRT images of interest are indicated.

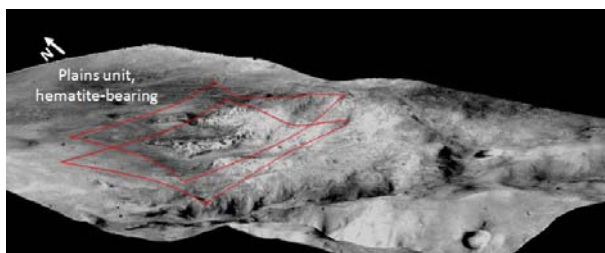


Figure 4. CTX P16\_007348\_1768 draped on MOLA topography, with a vertical exaggeration of 10. CRISM FRT footprints shown in Figure 3 are indicated in red.

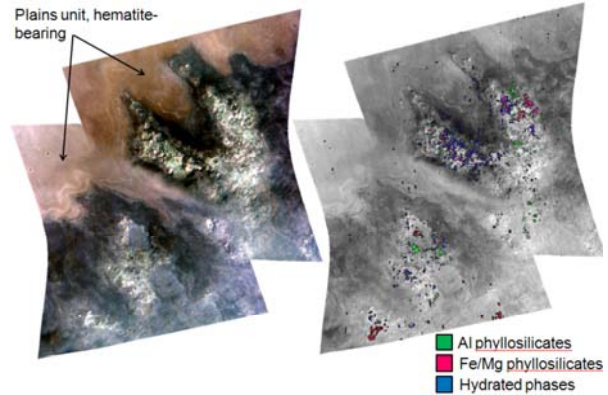


Figure 5. CRISM false color IR composite showing FRT 91c5 and FRT a063 (R=2.5, G=1.5, B=1.1 $\mu$ m) (left) and spectral index [14] composite (R=D2300, G=B2200, B=BD1900) (right).

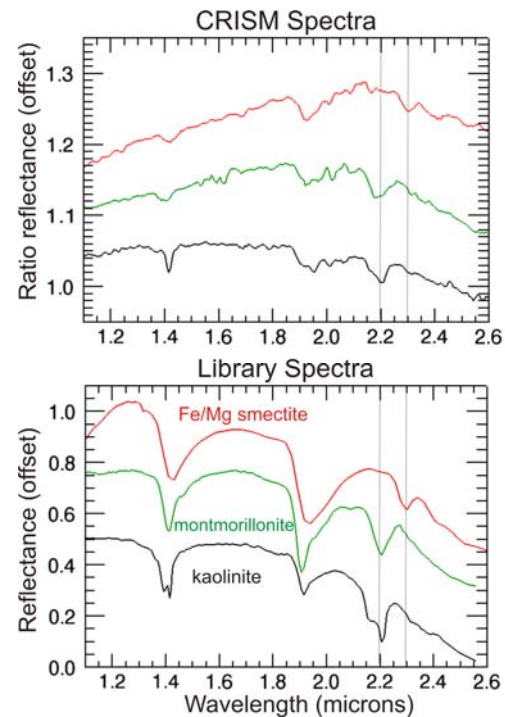


Figure 6. CRISM spectra extracted from areas indicated with arrows in Fig. 5 compared to library spectra.

**References:** [1] M. Malin and K. Edgett, (2000) *Science*, 288. [2] P.R. Christensen and S.W. Ruff (2004) *JGR*, 107. [3] J.-P. Bibring et al. (2004) *Mars Express: The Scientific Payload*, p37-49. [4] S. Murchie et al. (2007) *JGR*, 112. [5] F. Poulet et al. (2005) *Nature*, 438. [6] F. Poulet et al. (2008) *Icarus*, 195. [7] A. Gendrin et al. (2005) *Science*, 307. [8] S.M. Wiseman et al. (2007) *LPS XXXIX*, #1806. [9] S.M. Wiseman et al. (2008) *GRL*, submitted. [10] R.E. Arvidson et al. (2003) *JGR*, 108. [11] K.S. Edgett (2005) *Mars*, 1. [12] D. Loizeau (2007) *JGR*, 112. [13] J.C. Andrews-Hanna and M.T. Zuber (2008) *LPS XXXIX*, 1993. [14] S.M. Pelkey et al. (2007) *JGR*, 112.